ORIGINAL ARTICLE

Psychiatry and Clinical Psychopharmacology 2021;31(1):48-59
DOI: 10.5152/pcp.2021.20181

Modeling Schizophrenia with Glioblastoma Cells: In Vitro Analysis of Risperidone Treatment on Glial Spheroids

Ozge Sezin Somuncu[1], Irem Karaman[1], Hilal Piril Saracoglu[2], Erdem Yilmaz[3], Demet Akin[4]

[1]Department of Pathology, Stony Brook Medicine, New York, USA; [2]Cellular and Molecular Medicine, Institute of Health Sciences, Koç University, İstanbul, Turkey; [3]Department of Biochemistry, Bahçeşehir University School of Medicine, İstanbul, Turkey; [4]Department of Pharmacology, Bahçeşehir University School of Medicine, İstanbul, Turkey

ABSTRACT

Objective: Glioblastoma is the most malicious type of glioma presenting a genetic background via diverse mutations and exhibits differential sensitivity to treatment. Meanwhile, schizophrenia is a heterogeneous disease with a complex etiology. Studies report an elevation in pro-inflammatory cytokines in patients with schizophrenia and changes in biochemical metabolism. In the present study, the tumor spheroid technology is applied to two different glioblastoma lines which resemble schizophrenia manifestation along with the investigation of the potential anti-tumor effect of an atypical antipsychotic drug, risperidone. Our hypothesis built on case reports showing patients with schizophrenia being treated with risperidone that turned out to have glioblastoma in post-mortem evaluation. Risperidone has been suggested to carry therapeutic effects for glioblastoma and elongated lifespan after the diagnosis of cancer.

Materials and Methods: In this current study, 3D models using C6 and U87 glioblastoma cells and monocytes for representing the disease grown as multicellular spheroids were established. Spheroids were treated with the anti-schizophrenic agent risperidone and indicated almost similar results to the clinics suggesting that glioblastoma and schizophrenia share mutual physiological characteristics.

Results: U87 and C6 spheroid systems were analyzed molecularly after the treatment of risperidone where U87 spheroid models were found highly resembling the overall behavior of schizophrenia. This present work correlated the stated two diseases in molecular level to encourage the efforts for personalized medicine.

Conclusion: The anti-tumor effects of risperidone on glioblastoma is not very well established yet. It should not be missed that a picture of schizophrenia in clinics may be the result of an underlying lesion in a specific brain area. Thus, especially schizophrenia patients who may be at risk for developing brain tumors should be further investigated and treated accordingly.

ARTICLE HISTORY

Received: 15 November, 2020
Accepted: 21 January, 2021

KEYWORDS: Glioblastoma, risperidone, schizophrenia, spheroids, three-dimensional cell culture

INTRODUCTION

Schizophrenia is defined as a chronic brain disorder that affects the individual's way of thinking, feeling, and behavior.[1] According to WHO 2018 reports, more than 23 million people worldwide are diagnosed with the disease.[2] Depending on the variability in brain malformations, there are several clinical findings of schizophrenia such as positive symptoms (delusions and hallucinations), negative symptoms (affective flattening, amotivation, and anhedonia), and cognitive symptoms (disorganized speech and cognitive deficits).[3] These psychiatric symptoms can also manifest to patients with organic brain lesions in neurologically silent brain areas.[4]

Genetics, neurodevelopmental deficiencies, neurotransmitter imbalance, and birth complications can be the underlying causes of schizophrenia. Although no single gene is directly responsible, schizophrenia tends to run in families which leads to the abnormal expression of several genes involved in the disease.[5] In addition, imbalance in the levels of the two neurotransmitters dopamine and serotonin is typically seen in patients with the disease.[6] Meanwhile, genetic description of schizophrenia is often associated with stigmatizing attitudes.[7]

In a cellular point of view, among many others, the dysregulation of immune progression in the central nervous system (CNS) is suggested as an underlying disease mechanism. Resident microglia and perivascular and invading macrophages are the key elements in the CNS immune system, which release proinflammatory

Corresponding author: Ozge Sezin Somuncu, E-mail: ozge.somuncu@stonybrook.edu

Cite this article as: Sezin Somuncu O, Karaman I, Piril Saracoglu H, Yilmaz E, Akin D. Modeling schizophrenia with glioblastoma cells: In vitro analysis of risperidone treatment on glial spheroids. *Psychiatr Clin Psychopharmacol*. 2021; 31: 48-59.

mediators and may give rise to neuronal dysfunction that is responsible for disease progression.[8] In general, a significant disturbance of this molecular network, in which one dysregulation induces another, constitutes the background of the disease.[9]

Morphologically, altered brain structures of schizophrenic patients are observed to be static and non-progressive throughout the disease. Enlargement of the lateral ventricles and reductions in the volume of the areas in the cerebral cortex are some prominent morphological changes of schizophrenic patients' brain. While hippocampal neuropathology studies, although inconsistent, signify a decreased volume and abnormal synaptic connectivity in the hippocampus of schizophrenic patients, cortical neuropathology studies also reported an increased neuronal compactness in the prefrontal cortex.[10] Depletion of grey matter in the cerebellum and superior temporal gyrus may be inferred as early onset markers, whereas grey matter reduction in the anterior cingulate are indicators of genetic psychosis.[11]

Bunevicius et al.[4] mentioned three patients who had 3-10 years antiquities of schizophrenia spectrum conditions and were eventually diagnosed with glioma in the left temporal lobe. They have concluded that decrease in grey matter volume of the left temporal lobe due to the mass might be the reason for schizophrenia.[4] Supportively, Faraz et al.[12] reported that long-term survival from glioblastoma could be related to the anti-tumor effect of risperidone use for paranoid schizophrenia through dopamine receptor D2 (D2R) and serotonin receptor 7 (5-HT7R) antagonism.[12] Although other studies suggest that schizophrenia patients have a lower incidence of glioma, it is unclear whether the tumor can constitute a clinical picture of schizophrenia or vice versa.[13]

Tumor spheroids establish an operative 3D in vitro model to explore the avascular stage of tumor development to mimic the microenvironment and tumor heterogeneity. Considerations such as gene expression, cell morphology, neuronal excitability, synapse formation, and characteristics of the microenvironment can be analyzed in this model to further our understanding of some illnesses including schizophrenia so that it can be utilized as a drug discovery platform.[14]

The aim of the study was built on the idea of whether the glial dysfunction has a similar attendance to both schizophrenia and glioma and whether risperidone has an anti-tumor effect.[12] According to the reference study, pro-inflammatory cytokine increments and elevated TOS levels have resembled the schizophrenia picture in the C6 glioma cells.[12] In the present study, the tumor spheroid technology is applied to two different glioblastoma lines that resemble schizophrenia manifestation, along with the investigation of the potential anti-tumor effect of the atypical antipsychotic drug risperidone.

MATERIALS AND METHODS

U87 and C6 Glioblastoma Culture

U87 and C6 cell lines were bought from the American Type Culture Collection (ATCC, USA). U87 and C6 glioblastoma cells were cultured in DMEM (Gibco/Invitrogen) media supplemented with 10% (v/v) heat-inactivated FBS and 1% penicillin/streptomycin solution. THP-1 (human monocytic cell line) was ordered from ATCC and was grown in RPMI-1640 (+) L-glutamine supplemented with 10% FBS and 1% penicillin/streptomycin solution (Gibco/Invitrogen). For passaging, cells were centrifuged at 1200 rpm for 5 min in order to precipitate the cells. Media, which is collected as supernatant, was discarded and the obtained cells were resuspended in media. Cells were then placed into a T-75 flask containing 15 mL media. Cells were incubated at 5% CO_2 at 37°C for two days. After two days incubation, the present media was switched to fresh media. Cells were left to grow until they gained 80% confluency.[15] For C6 cell culturing, the same procedure was followed with DMEM (Gibco/Invitrogen) media complemented with 10% (v/v) heat-inactivated FBS and 1% penicillin/streptomycin.[16] For THP-1 cells, cultures were established by centrifugation with subsequent resuspension at 2×10^4 viable cells/mL.[17]

Generation of Glioblastoma Spheroids

The media was removed, and cells were washed with 1 mL of D-PBS without calcium and magnesium solution. Resuspension was completed in 1 mL of trypsin/EDTA and then cells were incubated for 2 min at 37°C. Matrigel droplets were prepared in a culture dish as 50 µL bubbles including glioblastoma cells and immune progenitor cells. Excess medium was removed by a vacuum device. Bubble containing dishes were placed into the 37°C incubator and left for 20-30 min. MEM for U87 and DMEM for C6 were added to the bubble-containing wells. The cells were incubated for 3 weeks by changing the media every two days to reach an adequate size. At the end of week 3, glioblastoma spheroids were harvested, fixed, and processed for further analysis.[18] The workflow of the spheroid generation can be observed in Figure 1A.

Microscopical Analysis of Formed Spheroids

Microscopical examination was conducted to show the growth and necrosis analysis of spheroids; 8 mm of the thin end of 200 µL pipette tips were cut for expanding the space width to transfer the molded structures into 400 µL DMEM in 24-well plates. Spheroids were visualized both at week 2 and week 4 in 40× magnification by ZEISS inverted microscope.[19] The area, mean, and length of both types of spheroid systems were measured by using the microscope-attached measurement software LAS-X Life Science (Leica Microsystems, USA). Analysis of the visual properties of

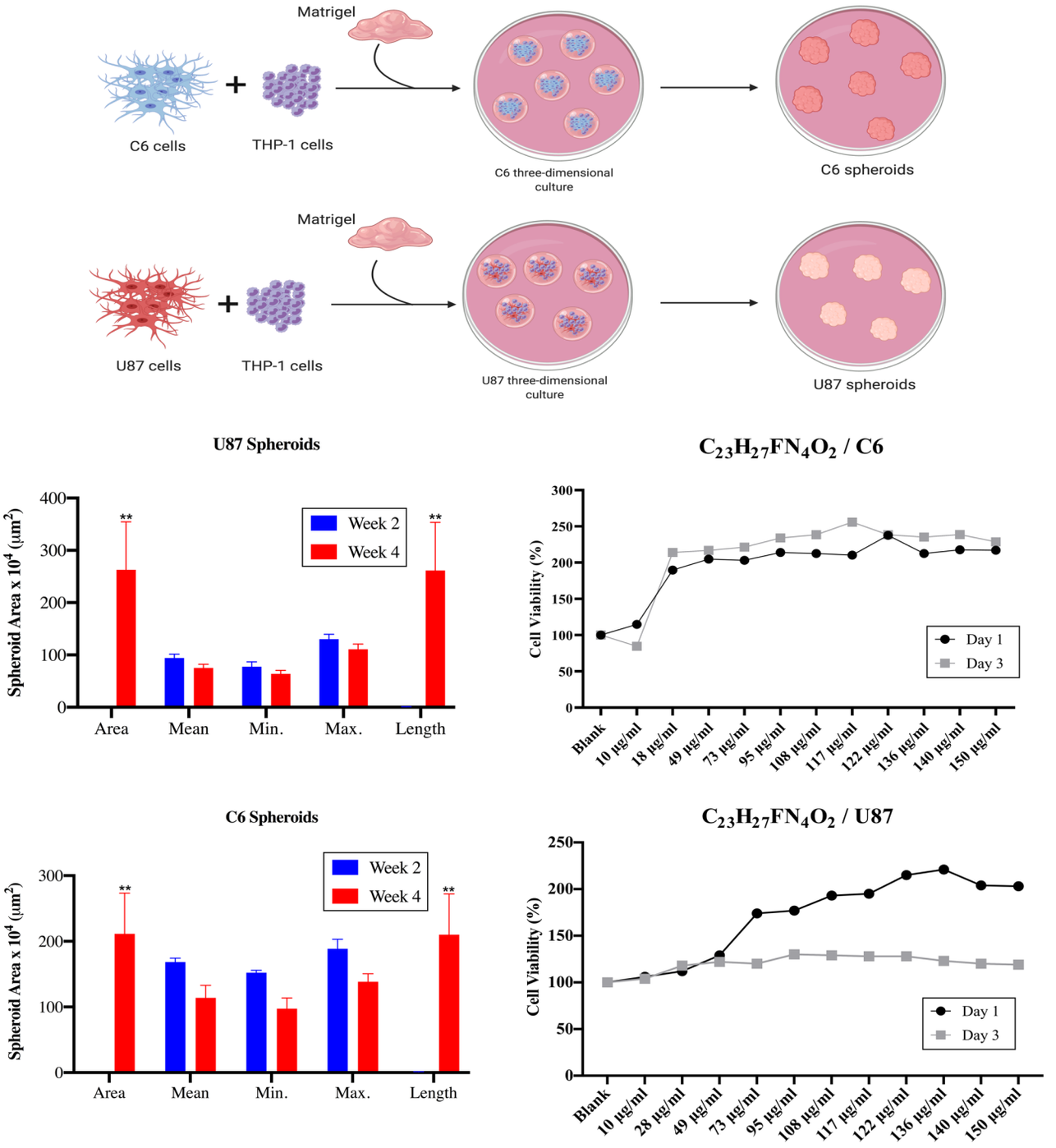

Figure 1. Spheroid production and viability confirmation. (A) Workflow of the spheroid generation. Image created with BioRender. (B) Average spheroid sizes by the attendance of area versus mean, minimum, and maximum through length analysis completed by measurement software LAS-X Life Science (Leica Microsystems, USA). The sizes of the organoids were captured lastly in week 4 once the spheroids reached their maximum size before the internal cells die because of the lack of nourishment and physical tightness. µm², square micron; min., minimum size; max., maximum size. (**P < .01). (C) Cell viability for both C6 and U87 cells were established by colorimetric measurements of the reduction product of 3-[4,5-dimethylthiazol-2-yl]-2,5-diphenyltetra-zolium bromide (MTT). Cell viabilities were calculated as a percentage of the blank (no-risperidone treatment) over a concentration range of 10-150 µg/mL for both day 1 and day 3. The data represent the mean values ± SD (n=3).

organoids were competed statistically by GraphPad Prism 8 software.

Cell Viability Assay

Cell viability assay was performed to determine the highest non-toxic dose of risperidone. Formed spheroids were treated with various concentrations of risperidone ($C_{23}H_{27}FN_4O_2$) and the cell viabilities were analyzed by MTT assay both on day 1 and day 3. Risperidone concentrations were selected as indicated: 10 µg/mL, 28 µg/mL, 49 µg/mL, 73 µg/mL, 95 µg/mL, 108 µg/mL, 117 µg/mL, 122 µg/mL, 136 µg/mL, 140 µg/mL, and 150 µg/mL. The MTT assay procedure started with discarding media from the cell culture. After addition of 50 µL of serum-free media and 50 µL of MTT (3-(4,5-dimethylthiazol-2-yl)-2,5-diphenyl tetrazolium bromide) solution into each well, plates were incubated at 37°C for 3 h. Additional 150 µL of MTT solvent was added and plates were wrapped in foil. After the incubation, plates were placed in a shaker for 15 min. Absorbance of plate contents were read at OD_{590}.[20]

Quantitative Real-Time PCR Analysis for the Detection of Gene Expression

Quantitative real-time PCR analysis was performed to show the relative mRNA expression of the selected genes in different experimental groups. Risperidone-treated and non-treated spheroids were harvested without disturbing the tissue by using pipette tips. Spheroids were then centrifuged and washed with PBS. The RNA isolation procedure was conducted according to the RNAeasy Mini Kit (Qiagen, Germany). Samples were lysed and homogenized. The lysate was then added onto the RNAeasy silica membrane provided by the kit.[21] Subsequently, cDNA synthesis was completed via a high capacity cDNA reverse transcription kit (ThermoFisher, USA). For the cDNA synthesis reaction, the RT master mix was utilized. Each well received 10 µL of 2x RT master mix and 10 µL of RNA samples were placed. The RT master mix includes 10X RT buffer, 25X dNTP mix, primers, reverse transcriptase, RNase inhibitor, and nuclease-free H_2O. Plates were sealed and after small centrifugation they are loaded to the thermal cycler for cDNA synthesis.[22] For the investigation of *MMP-2*, *IL-6*, *TNF-a*, *TGF-B*, *IGF-1*, and *LC3B*, quantitative real-time PCR analysis was done similar to the reference study.[23] As an internal control *GAPDH* was used. Primer sequences used for each transcript can be observed in Table 1.

Total Glucose Measurements

The total glucose assay was conducted for direct measurement of glucose in different experimental groups. For total glucose measurements, total glucose assay kit (Abcam) was utilized according to the instructions of the kit; 50 µL of the reaction mix was prepared and added into each well. Additionally, 50 µL of the background reaction mix was added into the sample background control wells. Samples were mixed and protected from light throughout the incubation for 30 min at 37°C. Measurement of the plates was done with optical density at 540 nm.[24]

Total Cholesterol Assay

Total cholesterol assay was performed for determining the total cholesterol in media of the different spheroid systems treated with risperidone. Parallel to the prior assays, total cholesterol analysis was conducted according to the kit (Elabscience) instructions. Cell suspension was centrifuged at 1000*g* for 10 min. The supernatant was discarded, and the sediment was preserved. Then, the sediment was washed with iso-osmia buffer (0.1 mol/L, pH 7-7.4 phosphate buffer) for 1-2 times and was centrifuged at 1000*g* for 10 min. The supernatant was discarded again and 0.3-0.5 mL of homogenate medium was added at a ratio of cells. Samples were subjected to ultrasonic treatment in an ice water bath (power: 300 W, 3-5 sec/time, interval for 30 sec, 3-5 times) or grind with hand-operated; 10 µL of

Table 1. Primer Sequences Used for Real-Time PCR Analysis

Names of the Genes	Primer Sequence (5′-3′)
MMP2	Forward Primer: AGCGAGTGGATGCCGCCTTTAA
	Reverse Primer: CATTCCAGGCATCTGCGATGAG
IL-6	Forward Primer: AGACAGCCACTCACCTCTTCAG
	Reverse Primer: TTCTGCCAGTGCCTCTTTGCTG
TNF-a	Forward Primer: CTCTTCTGCCTGCTGCACTTTG
	Reverse Primer: ATGGGCTACAGGCTTGTCACTC
TGF-B	Forward Primer: TACCTGAACCCGTGTTGCTCTC
	Reverse Primer: GTTGCTGAGGTATCGCCAGGAA
IGF-1	Forward Primer: CCGAGACACGCTCCATCCAC
	Reverse Primer: GTGGGGTGGGACAGAAGTGC
LC3B	Forward Primer: GAGAAGCAGCTTCCTGTTCTGG
	Reverse Primer: GTGTCCGTTCACCAACAGGAAG

All primers were designed by our group. The primers were designed with annealing temperature of 60°C.

double distilled water was added into a 2 mL tube for the blank tube; 10 µL of reagent 2 was added to the standard tube; 10 µL of Samples were then added into tubes individually. Afterwards, 1000 µL of reagent 1 was added to each tube and mixed. Finally, all tubes were incubated at 37°C for 10 min and then the samples were analyzed with optical density at 570 nm.

Total Bilirubin Assay

Total bilirubin assay was performed for establishing total cholesterol in media of different spheroid systems treated with risperidone. Bilirubin assay was conducted with the bilirubin (total and direct) colorimetric assay kit (Abcam). In accordance with the directions found in the kit,[25] bilirubin standard (150 µL of 0.2 µg/µL) was diluted in 150 µL of 100% DMSO. In order to produce a standard curve, dilution was assembled by using 0.2 µg/µL intervals. Samples were prepared by placing into the wells with necessary DMSO. For the reaction mix, 20 µL of bilirubin reagent 1, 5 µL of bilirubin reagent 2, and 100 µL of catalyst were used. Upon 125 µL of reagent mix preparation, the well plate was incubated for 30 min at room temperature. A second incubation was done for 20 min at room temperature with light protection following the addition of 75 µL of total bilirubin probe to all standards, samples, and background control. Finally, the plates were measured with an optical density at 530 nm.

Total Antioxidant and Total Oxidant Status Assay

Total Antioxidant Status (TAS) Assay Kit (Sigma-Aldrich) was used and the kit protocol was followed for TAS determination; 1 mM Trolax standard solution was used for making a standard curve by setting up different dilutions; 100 µL of Cu^{2+} working solution was added to each well containing standards and samples. Thereafter, wells were mixed and incubated at room temperature for 90 min. The plate was then transferred to a microplate reader to be analyzed at OD 570 nm.[26] Media of the samples for the measurement of total oxidant status (TOS) were stored at -80°C until needed. TOS was examined by Erel's TOS method[27], which is about the oxidation of ferrous ion to ferric ion in the presence of diverse oxidative species in the acidic medium. Ferric ion was analyzed by xylenol orange. Concisely, xylenol orange, NaCl, and glycerol in a H_2SO_4 solution were incubated with the samples for 3 min. Consequently, ferrous ion and *o*-dianisidine in H_2SO_4 were applied to the reaction. The alteration in absorbance was examined, and the results were analyzed by a standard curve of H_2O_2 solution and expressed in µmol/L.[27]

Fluorescent Immunohistochemistry Analysis

Fluorescent immunohistochemistry was employed for showing the differential protein expression of selected antibodies in different spheroid systems treated with risperidone. Expression patterns of G-protein g(q), alpha subunit (GAQ), nuclear factor kappa B (NF-κB), and phosphoinositide phospholipase C (PLC3) were selected for the immunofluorescence assay. OCT (Agar Scientific) embedded organoids were sectioned in 5 µm thickness. Samples were incubated overnight in PBS-5% FBS at 4°C with primary antibodies. Thereafter, sections were rinsed and incubated for 1 h at room temperature with Alexa Fluor-conjugated secondary antibodies. Microscopical analysis and imaging were performed on a Leica DMLB Phase Contrast Fluorescence Microscope.[28]

Statistical Analysis

Complete data were presented as means with standard errors (SD). Graphics were drawn via GraphPad Prism 8 software (GraphPad Prism, USA). The statistical inquiry of the grades was completed by using one-way ANOVA trailed by multiple-comparison Tukey's tests with GraphPad Prism 8 software. Asterisks indicate levels of significance. When a *P*-value was found less than 0.05, it is flagged with an asterisk (*) when found less than 0.01, it is flagged with two asterisks (**). If a *P*-value was less than 0.001, it is flagged with three asterisks (***).[29] Heat maps representing gene expression were generated from quantitative real-time PCR and clustered by using complete linkage of Heatmapper software showing both column and row dendrogram for hierarchical clustering.[30] Row Z-scores were demonstrated as blue for high values and red for low values, respectively.

RESULTS

Microscopical Examination and Comparison of Spheroids

The U87 and C6 spheroids were compared according to the content of area, mean, and length. U87 spheroids exhibited higher growth and a healthier development with no indication of necrosis in week 4 samples. U87 spheroids were found better integrated and better shaped of rosette formation in terms of generating healthier neural circuits when compared with C6 spheroids. U87 spheroids constituted a regulated system for disease modeling and drug testing. Two more weeks of growth in culture systems found to be more effective on U87 models where the same difference effected C6 model's growth slightly. Mean values, which suggest healthy growth by size, were found decreased in C6 systems less than the U87 ones when cultured two more weeks (Figure 1B).

Cell Viability Assay

In order to determine the highest non-toxic dose of risperidone ($C_{23}H_{27}FN_4O_2$) on U87 and C6 cells, 11 different concentrations of risperidone were employed. After dose-dependent risperidone application, cell viability assay was performed for day 1 and day 3 to find the optimal dose of the drug for further experimentation. As indicated in Figure 1C, C6 cells indicated a peak treated once with 10 µg/mL of risperidone, where the highest non-toxic dose

was found as 117 µg/mL in day 1 samples. Overall data showed that the best possible dosage for risperidone on C6 cells was 122 µg/mL since for day 3 it was the highest non-toxic dose and even in day 1 the viability was one of the most effective ones. Day 1 and day 3 cell viability profiles were found dissimilar to U87 cells. Day 1 profile indicated the highest non-toxic dose as 136 µg/mL. However, day 3 profiles indicated lower cell viabilities for all the doses when compared to day 1 profile; 122 µg/mL was selected to further analyze U87 cells since it was one of the optimal doses on both day 1 and day 3 results.

Gene Expression Analysis

Quantitative analysis of PCR products showed that the densitometrical units of *MMP-2* were found as $M=0.5228$, $SD=0.0905$ for U87 spheroid, $M=0.90051$, $SD=0.15597$ for U87 sph./risp., $M=0.2936$, $SD=0.0508$ for C6 spheroid, and $M=0.3623$, $SD=0.06276$ for C6 sph./risp. *MMP-2* expression almost doubled when treated with risperidone in U87 spheroids. Risperidone treatment was found to carry an insignificant effect on *MMP-2* expression for C6 spheroid systems. *TGF-ß1* expression in densitometrical units were detected as $M=0.05078$, $SD=0.00879$ for U87 spheroid, $M=0.4270$, $SD=0.0739$ for U87 sph./risp., $M=0.2532$, $SD=0.0438$ for C6 spheroid, and $M=0.2268$, $SD=0.03992$ for C6 sph./risp. Risperidone treatment increased *TGF-ß1* expression in U87 spheroid systems more than 8-fold. The expression of *TGF-ß1* for C6 spheroid systems was found unaffected from risperidone treatment. *TNF-a* expressions were detected as $M=0.6824$, $SD=0.1182$ for U87 spheroid, $M=0.1888$, $SD=0.0327$ for U87 sph./risp., $M=0.3369$, $SD = 0.05836$ for C6 spheroid, and $M=0.64027$, $SD=0.11089$ for C6 sph./risp. In case of Risperidone treatment, *TNF-a* expression decreased almost 6 times. In contrast, C6 spheroids indicated 2 times higher expression when treated with risperidone. Densitometrical units of *LC3B* were found as $M=0.06565$, $SD=0.01137$ for U87 spheroid, $M=0.90058$, $SD=0.15598$ for U87 sph./risp., $M=0.09965$, $SD=0.01726$ for C6 spheroids and $M=0.35893$, $SD=0.06216$ for C6 sph./risp. LC3B expression was found significantly elevated for both spheroids when treated with risperidone (Figure 2).

Heat Map

In order to visualize relative differences in expression folds of C6 and U87 spheroids in non-treated and treated samples, a heat map was drawn. *MMP-2*, *IL-6*, and *LC3B* all shared a similar gene expression pattern, which has enhanced expression after treatment with risperidone in both types of glioblastoma spheroids. *TGF-ß* and *IGF-1* also shared similar gene expression patterns, which was diminished in C6 spheroids but increased in U87 spheroids after treatment. Hierarchical clustering of each gene group showed that *IL-6* and *MMP-2* indicated the maximum gene expression resemblances. *TGF-ß1* and *IGF-1* expression patterns were also found to correlate with both spheroid groups. The most irrelevant genes were detected as *TNF-a* and *IL-6* in schizophrenia models. *LC3B*, *MMP-2*, and *IL-6* expressions were found to be almost the same folds in risperidone treated U87 spheroids (Figure 2).

Total Glucose, Cholesterol, and Bilirubin Differences after Risperidone Treatment

Although both C6 and U87 risperidone-treated spheroids have shown higher total glucose levels after treatment, U87 spheroids showed statistically significant augmentation (Figure 3A). Risperidone treatment has caused a significantly decreased total cholesterol status in C6 spheroids. However, there was no significant effect of risperidone treatment on U87 spheroids (Figure 3B). The total bilirubin levels were reduced to one-seventh after treatment in U87 spheroids. While the U87 spheroids demonstrated a significantly diminished bilirubin level, the alteration in the total level of bilirubin in C6 spheroids were not significant (Figure 3C).

Total Oxidant and Total Antioxidant Assays

TOS and TAS were measured from the cell culture media in which the spheroids were grown. Specifically, treatment with risperidone decreased the TOS to one-half in C6 spheroids. TAS was significantly decreased once treated with risperidone. No statistically significant change was found in TAS for both C6 and U87 spheroids. However, even though it was insignificant, there was a slight decrease in TAS level for U87 spheroids when treated with risperidone (Figure 3D).

Fluorescent Immunohistochemistry Analysis

Given that G-protein g(q) alpha subunit (GAQ), nuclear factor kappa B (NF-kB), and phosphoinositide phospholipase C (PLC3) expressions are important in glial dysfunction in schizophrenia, the expression activation or suppression was determined with fluorescent IHC before and after treatment in both types of glioblastoma spheroids. GAQ showed higher expression after treatment in both spheroids, but significantly higher in the C6 line. Conversely, post-treatment NF-kB expression was significantly higher in both spheroids but especially in the U87 line. PLC3 indicated a similar expression pattern with NF-kB, and it was significantly higher in U87 spheroids after treatment, but not in the C6 line (Figure 3E).

DISCUSSION

Here we demonstrate the effects of risperidone which is being used for the treatment of schizophrenia[31] in glioblastoma spheroids. Our hypothesis belonged to a fact that there are case reports in the literature showing that schizophrenia patients being treated with risperidone

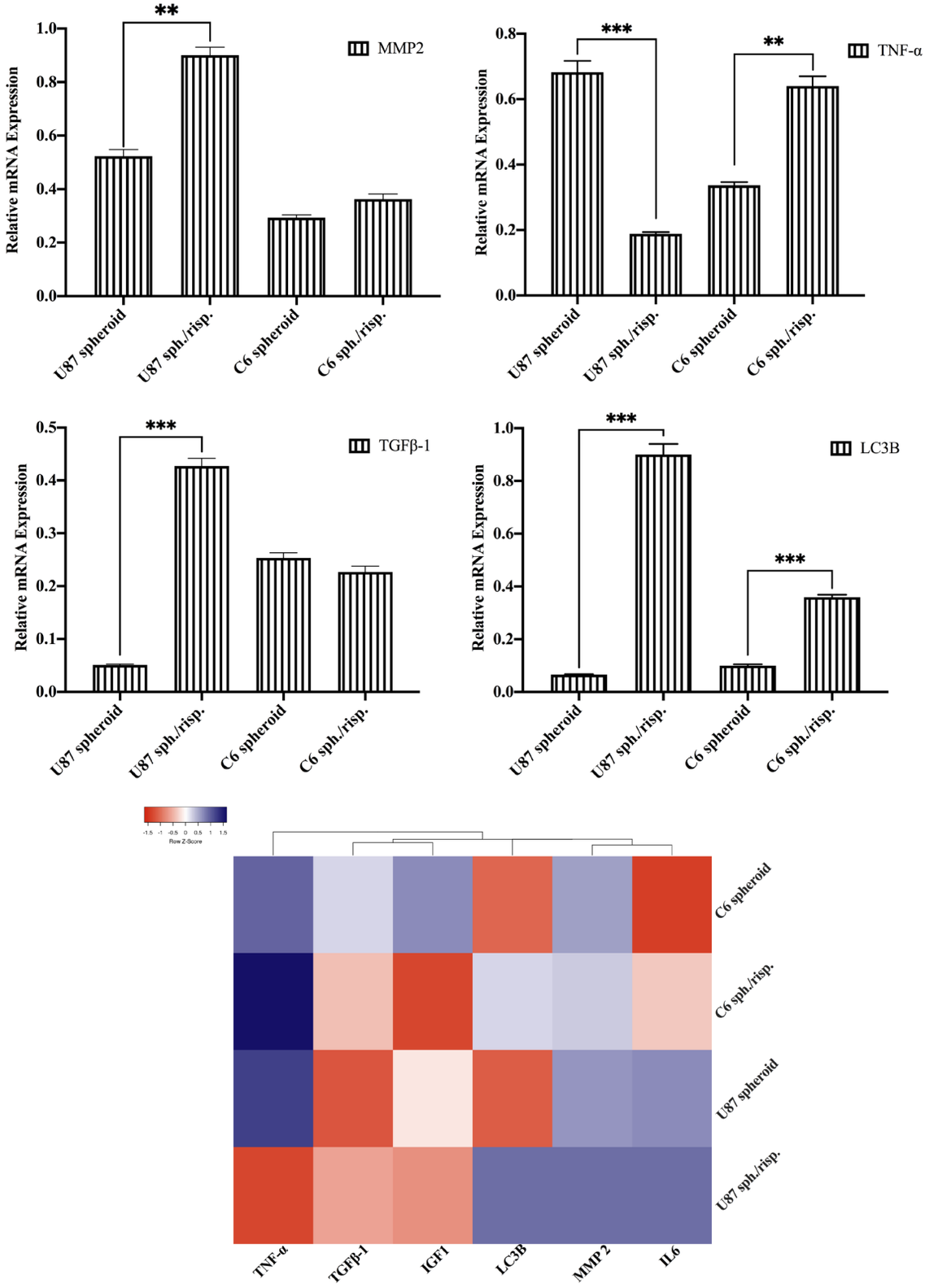

Figure 2. Gene expression analysis of U87 and C6 spheroids combined with the risperidone treated spheroids in each group. Heat map presenting the gene expression data for a range of genes analyzed by qPCR. A graph of quantitative RT-PCR MMP-2, TGF-ß1, TNF-α, and LC3B mRNA expression changes in comparison for each group. Abbreviations: MMP-2, matrix metalloproteinase-2; TGF-ß1, transforming growth factor beta 1; TNF-α, tumor necrosis factor-α; LC3B, microtubule-associated protein 1A/1B-light chain 3; qPCR, quantitative real time polymerase chain reaction. *P < .05, **P < .01, ***P < .001. Notes: Results were examined by one-way ANOVA and Tukey's posttest.

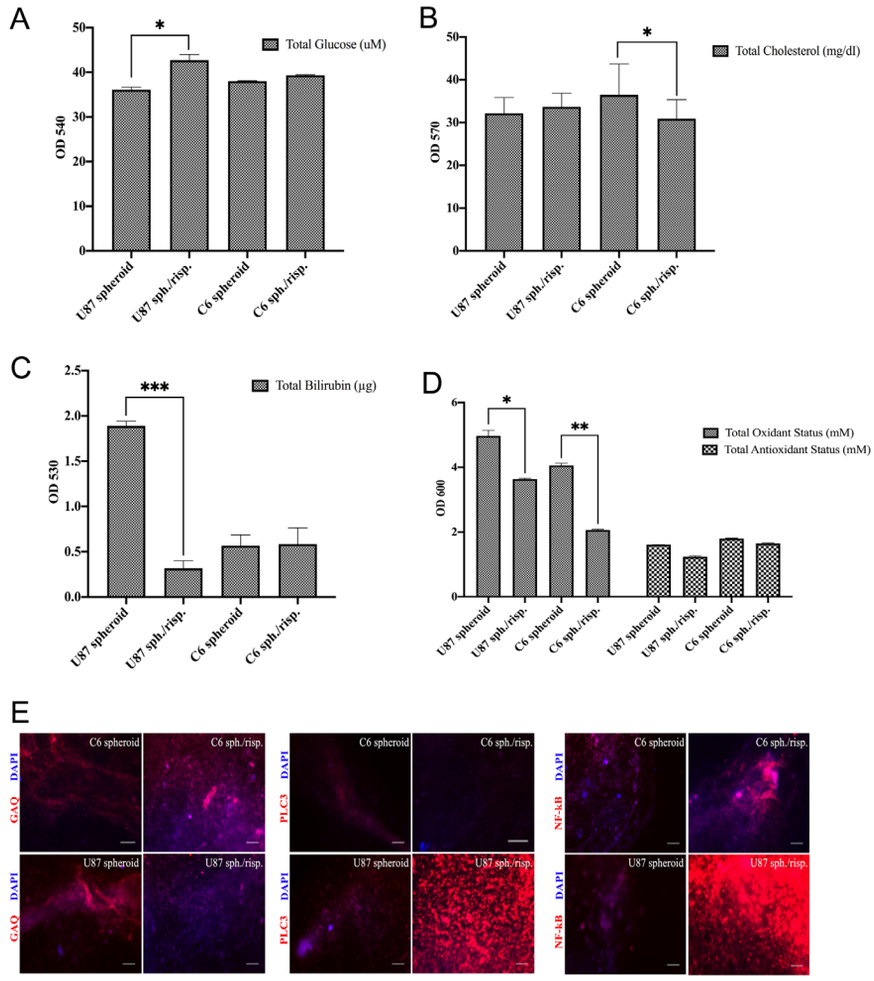

Figure 3. Biochemical quantification and protein expression profiles of spheroid cultures grown with and without risperidone treatment. (A) Colorimetric amount of total glucose in media of untreated U87 and C6 spheroids and treated ones. Analytical reading was performed in 540 OD. (B) Colorimetric analysis of total cholesterol in media of untreated U87 and C6 spheroids and the treated ones. The analytical reading was completed in 570 OD. (C) Colorimetric amount of total bilirubin in media of untreated U87 and C6 spheroids and risperidone applied ones. Analytical reading was performed in 530 OD. (D) TAS and TOS levels of media obtained from treated and untreated spheroid cultures. OD, optical density; TAS, total antioxidant status; TOS, total oxidant status; sph., spheroid; risp., risperidone. *P < .05, **P < .01, ***P < .001. Notes: Results were examined by one-way ANOVA and Tukey's posttest. (E) Fluorescence images of U87 and C6 spheroids before and after risperidone treatment by three different pathways of schizophrenia prognosis related antibodies GAQ, PLC3, and NF-κB. GAQ, PLC3, and NF-κB were stained with red individually, whereas DAPI was stained with blue in every section. GAQ, Gq protein alpha subunit; PLC3, phosphoinositide phospholipase C3; NF-κB, nuclear factor kappa B.

have experienced glioblastoma which was diagnosed post-mortem.[4] Previous reports suggest that risperidone may have been carrying a therapeutic effect for glioblastoma, and therefore elongates lifespan after cancer diagnosis.[32] Glial dysfunction in schizophrenia patients can be demonstrated by deviations in the expression levels of various essential molecules. In order to evaluate the effects, different molecular analysis protocols were applied in our study. Cell viability assay indicated that none of the risperidone doses were toxic for cells. Therefore, this gave us the idea that risperidone can be physically effective on cancer cells and affect cellular behavior/aggressiveness.

A pro-inflammatory molecule IL-6 acts context dependent, while it shows immunosuppressive properties by preventing action of the transcription factors or microbicidal activity of macrophages. It can also stimulate IL-1R antagonist and soluble p55 receptor, regulating TNF function.[33] Comparison of *TNF-a* among before and after treatment of schizophrenic patients revealed that treatment leads to a significant decrease in *TNF-a* levels.[34] According to a recent meta-analysis, IL-6 can be utilized as a stating marker for schizophrenia due to the fact that IL-6 levels in first-episode psychosis and acute relapse are increased.[33] Taken together with the immune system cells contained in spheroids, IL-6 expression was shown to be meaningfully higher after treatment in our study. This can be explained by the application of the drug in the early stage of the disease, mimicking a first-episode schizophrenia picture.

The relation between IL-6 and TNF-α seems to be context dependent, while IL-6 can be considered to induce TNF-α expression in the C6 line, and their expression patterns were opposite to each other in the U87 line.

The samples taken from patients with malignancies in the CNS and neuropathological disorders, like glioblastoma and schizophrenia, revealed elevated *TGF-β* levels.[35] For the neural stem cell maintenance, differentiation, and growth, *TGF-β* signaling is essential. Evaluation of the results in the light of this knowledge showed that even though there is a slight decrement in the C6 line after treatment, there is high increment in treated U87 spheroids. Since TGF-β is a regulatory cytokine, it is reported to be increased after treatment in patients with first episode psychosis, while it is decreased in schizophrenia patients, which is consistent with our data. It is also stated that as a pleiotropic cytokine, TGF-β plays an immunosuppressive role in the early stages of illness.[36]

MMP-2 and MMP-9, which function by remodeling the extracellular matrix (ECM), have been mentioned in many CNS disorders by causing leakage of the blood-brain barrier, abnormal wound healing, inflammation, and cancer.[37,38] When both neuroinflammation and barrier dysfunction combined, where MMPs were involved in both processes, their expression can advance progression of various CNS disorders.[38] They are also crucial for the processing of several proteins associated with synaptogenesis, synaptic plasticity, and long-term potentiation.[39] *MMP-2* is one among the schizophrenia-related genes and is shown to be upregulated in the patients.[40] Risperidone treatment seems to act through *MMP-2* activation.[41] As a result, increased expression in risperidone-treated spheroids were expected, and when compared, the increment in U87 spheroids was more significant than in the C6 line. As a transcription factor, *NF-κB* implicates in cell endurance, neuronal progression, and synaptic plasticity and knock-out mice studies establish discriminatory memory shortfalls. As reported, NF-κB levels were significantly diminished in the schizophrenic patients' brains.[42] Fluorescent IHC images affirmed that both the post-treatment spheroids showed a higher expression.

Disruption of *IGF-1* levels mostly causes schizophrenia via producing shortages in early periods of neurodevelopment, and low *IGF-1* intensities are linked with pre/postnatal growth and schizophrenia. Spheroids produced from different cell types exhibited contradicting results. In C6 risperidone-treated spheroids, decreased *IGF-1* levels were seen whereas there was an increment in the U87 line. However, decrement in C6 spheroids was more significant than U87 spheroids' increment. The reason why U87 spheroids have shown a different result than expected is questionable. Considering increased *TGF-β* in this U87 system, this might be the result of co-occurrence of immune/glucose metabolism disturbances which is seen in schizophrenic patients.[43]

LC3B is involved in autophagy machinery, and levels of activity-dependent neuroprotective protein, a molecule interacting with LC3B, were observed as increased in postmortem hippocampal samples from schizophrenia subjects.[44] In a study done with risperidone and haloperidol treatment, it was observed that treatments increased the acidic vesicle number which was interpreted as autophagic vesicles.[45] Expression analysis reported that both C6 and U87 risperidone-treated spheroids' *LC3B* levels were increased which is a corroborative evidence that both, in the sense of *LC3B* expression, are useful models. The higher significance of U87 spheroids makes them more suitable for modelling.

Schizophrenia has been associated with high cholesterol levels.[46] It was revealed that first-episode, reasonably old, antipsychotic-naive patients with schizophrenia had advanced intensities of plasma glucose, insulin, and cortisol than age- and sex-matched control subjects.[47] Murashita et al.[48] demonstrated that risperidone-treated patients also show higher blood glucose levels than controls, which was consistent with the results of the study.[48] The results obtained propose that C6 spheroids are better models compared to the U87 line in the sense of cholesterol levels. Schizophrenia patients have shown higher unconjugated bilirubin levels when compared with healthy individuals due to increased ROS levels.[49] Schizophrenic models treated with risperidone have lower bilirubin levels. Decrement of the total bilirubin levels after treatment revealed that the spheroids created from U87 were better models than C6 spheroids. Schizophrenia is convoyed by amplified lipid peroxidation and nitric oxide (NO) levels and by dropped antioxidant levels.[50] Previous studies revealed that schizophrenic patients have significantly lower plasma TAS while they demonstrate no alterations for TOS. While all subtypes of schizophrenia have lower TAS values than controls, paranoid schizophrenic patients show higher TAS values than the controls. These TAS/TOS level differences among schizophrenic patients and controls are said to be related to the defect in the antioxidant defense system.[51] The results propose that management with risperidone can have antioxidative effects by elevating PON1 (paraoxonase 1) and lowering LOOH (lipid hydroperoxides) levels.

A number of GPCRs (G-protein coupled receptors) covering D2R, serotonin 2 receptor (5-HT2), and metabotropic glutamate receptors have been associated with schizophrenia and to negative symptoms in particular. Moreover, it is reported that GPCR associated genes can be altered by antipsychotics.[52] Since it was expected that atypical antipsychotic compounds, have antagonistic effects on numerous neurotransmitter receptors and inhibit Gi- and Gq-dependent signaling, the reason why GAQ expression is

higher after treatment is questionable and should further be investigated on a molecular basis, especially in which particular pathway the drug triggers via GPCRs.[53]

PLCB1 and PLCB3 are molecules expressed extremely in tumor tissues in contrast to healthy tissues. Upon the stimulation of Gα protein ($G\alpha_{q/11}$ and or Gβγ), they are released, and their activation can increase intracellular calcium levels.[54] *TrkbPLC/PLC*-knock-in mice lacking *PLCγ1* docking sites validated the necessity of PLCγ1 activity for normal synaptic plasticity and associative memory.[55] In our study, U87-treated spheroids showed a significantly higher expression pattern while little to no difference was observed in C6 risperidone-treated spheroids. This may imply that U87 spheroids responded to risperidone better than the C6 spheroids.

The anti-tumor effects of risperidone on glioblastoma is not very well established yet. It should not be missed that a picture of schizophrenia in clinics may be the result of an underlying lesion in a specific brain area. We used the similarities of glioma and schizophrenia and tried to understand whether the schizophrenia medication risperidone has an anti-tumor effect. Schizophrenia patients who may be at risk for developing brain tumors should be further investigated for brain neoplasms and should be treated accordingly. An important limitation of studying schizophrenic patients with glioblastoma is that physicians generally realize the glioblastoma formation in the autopsy. Although tumor spheroids are new, studies using them are promising for the future of research and the clinic. Spheroids can only give information or the knowledge for the produced tissue types. Therefore, when a drug is tested on the spheroids, one cannot estimate the effects of the drug on another tissue which leads to the lack of knowledge on drug mechanism in whole body. Another limitation of this present study is that we tried to support glioblastoma cells with immune cells to mimic the microenvironment. However, since it was not a three-dimensional fully organized organoid system covering all the cell types effected by the medication, we only managed to reflect the disease and not fully mimic it. With advances in the spheroid and three-dimensional culture technologies, these limitations will hopefully be overcome. Overall, the common molecular fingerprints of both glioblastoma and schizophrenia was successfully demonstrated with this current study. This study may also be one of the few studies mimicking schizophrenia via glioma spheroids that was treated with risperidone for observing both anti-tumor and anti-schizophrenia effects of the medication.

Conflict of Interest: The authors declare that they have no conflict of interest.

Acknowledgements: We thank Türker Kılıç, Dean of Faculty, Bahçeşehir University Faculty of Medicine, for allowing the use of the research laboratories. We also thank Adam Naqvi and Sam Chiappone from Stony Brook University School of Medicine, Department of Pathology, for their efforts in proofreading.

Ethical committe Approval: Ethical committe approval was not required due to the design of this study.

Peer-review: Externally peer-reviewed.

Financial Disclosure: All the cells were bought from the American Type Culture Collection (ATCC, USA).

REFERENCES

1. Seppala J, Miettunen J, Jääskeläinen E, et al. Definition, epidemiology, clinical course and outcomes in treatment-resistant schizophrenia. *Eur Psychiatr*. 2017;41(S1):S67-S67. [CrossRef]
2. Charlson FJ, Ferrari AJ, Santomauro DF, et al. Global epidemiology and burden of schizophrenia: findings from the Global Burden of Disease Study 2016. *Schizophr Bull*. 2018;44(6):1195-1203. [CrossRef]
3. Stachowiak EK, Benson CA, Narla ST, et al. Cerebral organoids reveal early cortical maldevelopment in schizophrenia-computational anatomy and genomics, role of FGFR1. *Transl Psychiat*. 2017;7(11):6. [CrossRef]
4. Bunevicius A, Deltuva VP, Deltuviene D, Tamasauskas A, Bunevicius R. Brain lesions manifesting as psychiatric disorders: eight cases. *CNS Spectr*. 2008;13(11):950-958. [CrossRef]
5. Henriksen MG, Nordgaard J, Jansson LB. Genetics of schizophrenia: overview of methods, findings and limitations. *Front Hum Neurosci*. 2017;11:322. [CrossRef]
6. Modai S, Shomron N. Molecular risk factors for schizophrenia. *Trends Mol Med*. 2016;22(3):242-253. [CrossRef]
7. Serafini G, Pompili M, Haghighat R, et al. Stigmatization of schizophrenia as perceived by nurses, medical doctors, medical students and patients. *J Psychiatr Ment Hlt*. 2011;18(7):576-585. [CrossRef]
8. van Kesteren CFMG, Gremmels H, de Witte LD, et al. Immune involvement in the pathogenesis of schizophrenia: a meta-analysis on postmortem brain studies. *Transl Psychiat*. 2017;7(3):e1075. [CrossRef]
9. de Souza DF, Wartchow K, Hansen F, et al. Interleukin-6-induced S100B secretion is inhibited by haloperidol and risperidone. *Prog Neuro-Psychoph*. 2013;43:14-22. [CrossRef]
10. Rehn AE, Rees SM. Investigating the neurodevelopmental hypothesis of schizophrenia. *Clin Exp Pharmacol*. 2005;32(9):687-696. [CrossRef]
11. Fusar-Poli P, Smieskova R, Serafini G, Politi P, Borgwardt S. Neuroanatomical markers of genetic liability to psychosis and first episode psychosis: a voxelwise meta-analytical comparison. *World J Biol Psych*. 2014;15(3):219-228. [CrossRef]
12. Faraz S, Pannullo S, Rosenblum M, Smith A, Wernicke AG. Long-term survival in a patient with glioblastoma on antipsychotic therapy for schizophrenia: a case report and literature review. *Ther Adv Med Oncol*. 2016;8(6):421-428. [CrossRef]
13. Gao XC, Mi YJ, Guo N, et al. Glioma in schizophrenia: is the risk higher or lower? *Front Cell Neurosci*. 2018;12:289. [CrossRef]

14. Di Lullo E, Kriegstein AR. The use of brain organoids to investigate neural development and disease. *Nat Rev Neurosci*. 2017;18(10):573-584. [CrossRef]
15. Iacopino F, Angelucci C, Piacentini R, et al. Isolation of cancer stem cells from three human glioblastoma cell lines: characterization of two selected clones. *PLoS ONE*. 2014;9(8):e105166. [CrossRef]
16. Coyle DE. Adaptation of C6 glioma-cells to serum-free conditions leads to the expression of a mixed astrocyte-oligodendrocyte phenotype and increased production of neurite-promoting activity. *J Neurosci Res*. 1995;41(3):374-385. [CrossRef]
17. Aldo PB, Craveiro V, Guller S, Mor G. Effect of culture conditions on the phenotype of THP-1 monocyte cell line. *Am J Reprod Immunol*. 2013;70(1):80-86. [CrossRef]
18. Lancaster MA, Knoblich JA. Generation of cerebral organoids from human pluripotent stem cells. *Nat Protoc*. 2014;9(10):2329-2340. [CrossRef]
19. Mansour AA, Gonçalves JT, Bloyd CW, et al. An in vivo model of functional and vascularized human brain organoids (vol 36, pg 432, 2018). *Nat Biotechnol*. 2018;36(8):772. [CrossRef]
20. Bahuguna A, Khan I, Bajpai VK, Kang SC. MTT assay to evaluate the cytotoxic potential of a drug. *Bangl J Pharmacol*. 2017;12(2):115-118. [CrossRef]
21. Drost J, Karthaus WR, Gao D, et al. Organoid culture systems for prostate epithelial and cancer tissue. *Nat Protoc*. 2016;11(2):347-358. [CrossRef]
22. Blanco S, Bandiera R, Popis M, et al. Stem cell function and stress response are controlled by protein synthesis. *Nature*. 2016;534(7607):335-340. [CrossRef]
23. Somuncu S, Somuncu ÖS, Ballıca B, Tabandeh B. Deficiency of epithelial-mesenchymal transition causes child indirect inguinal hernia. *J Pediatr Surg*. 2020;55(4):665-671. [CrossRef]
24. Schnack L, Sohrabi Y, Lagache S, et al. Mechanisms of trained innate immunity in Oxldl and Bcg primed human coronary smooth muscle cells. *Atherosclerosis*. 2019;287:e24-e25. [CrossRef]
25. Park JB. N-Caffeoyltryptamine, a potent anti-inflammatory phenolic amide, suppressed MCP-1 expression in LPS-stimulated THP-1 cells and rats fed a high-fat diet. *Int J Mol Sci*. 2017;18(6):1148., PMID: 28555020 [CrossRef]
26. Miller NJ, Rice-Evans C, Davies MJ, Gopinathan V, Milner A. A novel method for measuring antioxidant capacity and its application to monitoring the antioxidant status in premature neonates. *Clin Sci*. 1993;84(4):407-412. [CrossRef]
27. Erel O. A new automated colorimetric method for measuring total oxidant status. *Clin Biochem*. 2005;38(12):1103-1111. [CrossRef]
28. Somuncu ÖS, Coşkun Y, Ballica B, Temiz AF, Somuncu D. In vitro artificial skin engineering by decellularized placental scaffold for secondary skin problems of meningomyelocele. *J Clin Neurosci*. 2019;59:291-297. [CrossRef]
29. labi BR, LaRanger R, Shay J, W. Decellularized mice colons as models to study the contribution of the extracellular matrix to cell behavior and colon cancer progression. *Acta Biomater*. 2019;100:213-222.
30. Babicki S, Arndt D, Marcu A, et al. Heatmapper: web-enabled heat mapping for all. *Nucleic Acids Res*. 2016;44(W1):W147-W153. [CrossRef]
31. Marder SR, Meibach RC. Risperidone in the treatment of schizophrenia. *Am J Psychiat*. 1994;151(6):825-835. [CrossRef]
32. Hendouei N, Saghafi F, Shadfar F, Hosseinimehr SJ. Molecular mechanisms of anti-psychotic drugs for improvement of cancer treatment. *Eur J Pharmacol*. 2019;856:172402. [CrossRef]
33. Borovcanin MM, Jovanovic I, Radosavljevic G, et al. Interleukin-6 in schizophrenia – is there a therapeutic relevance? *Front Psychiatry*. 2017;8:221. [CrossRef]
34. Ajami A, Abedian F, Hosseini SH et al. Serum TNF-α, IL-10 and IL-2 in schizophrenic patients before and after treatment with risperidone and clozapine. *Iran J Immunol*. 2014;11(3):200-209. [CrossRef]
35. Borovcanin M, Jovanovic I, Dejanovic SD et al. Possible role of TGF-beta pathways in schizophrenia. *Serb J Exp Clin Res*. 2015;17(1):3-8. [CrossRef]
36. Borovcanin M, Jovanovic I, Radosavljevic G, et al. Antipsychotics can modulate the cytokine profile in schizophrenia: attenuation of the type-2 inflammatory response. *Schizophr Res*. 2013;147(1):103-109. [CrossRef]
37. Liu XQ, Su P, Meng SS, et al. Role of matrix metalloproteinase-2/9 (MMP2/9) in lead-induced changes in an in vitro blood-brain barrier model. *Int J Biol Sci*. 2017;13(11):1351-1360. [CrossRef]
38. Rempe RG, Hartz AMS, Bauer B. Matrix metalloproteinases in the brain and blood-brain barrier: versatile breakers and makers. *J Cerebr Blood Met*. 2016;36(9):1481-1507. [CrossRef]
39. Domenici E, Willé DR, Tozzi F, et al. Plasma protein biomarkers for depression and schizophrenia by multi analyte profiling of case-control collections. *PLoS ONE*. 2010;5(2):e9166. [CrossRef]
40. Agarwal AB, Christensen AJ, Feng CY et al. Expression of schizophrenia biomarkers in extraocular muscles from patients with strabismus: an explanation for the link between exotropia and schizophrenia? *PeerJ*. 2017;5:e4214. [CrossRef]
41. Keilhoff G, Grecksch G, Bernstein HG, Roskoden T, Becker A. Risperidone and haloperidol promote survival of stem cells in the rat hippocampus. *Eur Arch Psy Clin*. 2009;260(2):151-162. [CrossRef]
42. Fu C, Chen D, Chen RJ, Hu QS, Wang GH. The schizophrenia-related protein dysbindin-1A is degraded and facilitates NF-kappa B activity in the nucleus. *PLoS ONE*. 2015;10(7):e0132639. [CrossRef]
43. Steiner J, Bernstein HG, Schiltz K, et al. Immune system and glucose metabolism interaction in schizophrenia: a chicken-egg dilemma. *Prog Neuro-Psychoph*. 2014;48:287-294. [CrossRef]
44. Merenlender-Wagner A, Malishkevich A, Shemer Z, et al. Autophagy has a key role in the pathophysiology of schizophrenia. *Mol Psychiatr*. 2015;20(1):126-132. [CrossRef]
45. Vucicevic L, Misirkic-Marjanovic M, Harhaji-Trajkovic L, Maric N, Trajkovic V. Mechanisms and therapeutic significance of autophagy modulation by antipsychotic drugs. *Cell Stress*. 2018;2(11):282-291. [CrossRef]

Q7

46. Woods AG, Sokolowska I, Taurines R, et al. Potential biomarkers in psychiatry: focus on the cholesterol system. *J Cell Mol Med*. 2012;16(6):1184-1195. [CrossRef]
47. van Nimwegen LJ, Storosum JG, Blumer RM, et al. Hepatic insulin resistance in antipsychotic naive schizophrenic patients: stable isotope studies of glucose metabolism. *J Clin Endocrinol Metab*. 2008;93(2):572-577. [CrossRef]
48. Murashita M, Inoue T, Kusumi I, et al. Glucose and lipid metabolism of long-term risperidone monotherapy in patients with schizophrenia. *Psychiat Clin Neuros*. 2007;61(1):54-58. [CrossRef]
49. Marques JG, Pedro I, Ouakinin S. Unconjugated bilirubin and acute psychosis: a five years retrospective observational and controlled study in patients with schizophrenia, schizoaffective and bipolar disorders. *Int J Psychiat Clin*. 2019;23(4):281-285., PMID: 31335268 [CrossRef]
50. Noto C, Ota VK, Gadelha A, et al. Oxidative stress in drug naive first episode psychosis and antioxidant effects of risperidone. *J Psychiatr Res*. 2015;68:210-216. [CrossRef]
51. Virit O, Altindag A, Yumru M, et al. A defect in the antioxidant defense system in schizophrenia. *Neuropsychobiology*. 2009;60(2):87-93. [CrossRef]
52. Chertkow Y, Weinreb O, Youdim MBH, Silver H. Gene expression changes in peripheral mononuclear cells from schizophrenic patients treated with a combination of antipsychotic with fluvoxamine. *Prog Neuro-Psychoph*. 2007;31(7):1356-1362. [CrossRef]
53. Mirnics K, Middleton FA, Stanwood GD, Lewis DA, Levitt P. Disease-specific changes in regulator of G-protein signaling 4 (RGS4) expression in schizophrenia. *Mol Psychiatr*. 2001;6(3):293-301. [CrossRef]
54. Wang XK, Huang KT, Zeng XM, et al. Diagnostic and prognostic value of mRNA expression of phospholipase C beta family genes in hepatitis B virus-associated hepatocellular carcinoma. *Oncol Rep*. 2019;41(5):2855-2875. [CrossRef]
55. Yang YR, Jung JH, Kim SJ, et al. Forebrain-specific ablation of phospholipase C gamma 1 causes manic-like behavior. *Mol Psychiatr*. 2017;22(10):1473-1482. [CrossRef]